Supplementary Materials

Structure Analysis and Luminescence Properties of Octaethyl(pyrene-tetrakis(biphenyl))tetrakis-(phosphonate)

Aysenur Limon,† Marcus N. A. Fetzer,† Christoph Janiak*

Institut für Anorganische Chemie und Strukturchemie, Heinrich-Heine-Universität Düsseldorf, 40204 Düsseldorf, Germany

† These authors contributed equally.

* Correspondence author

E-Mail: Christoph Janiak - janiak@uni-duesseldorf.de

Tel: +49-211-81-12286

E-mails: Aysenur Limon – aysenur.limon@hhu.de; Marcus N. A. Fetzer – fetzer@hhu.de;

Content

S1. Sources of chemicals **S2**

S2. Conventional synthetic route of aromatic phosphonates **S3**

S3. NMR spectra **S4**

S4. MS spectra **S8**

S5. X-ray structure of compound Et_8-PyTPPE **S9**

S6. π-π stacking and C–H···π interactions **S11**

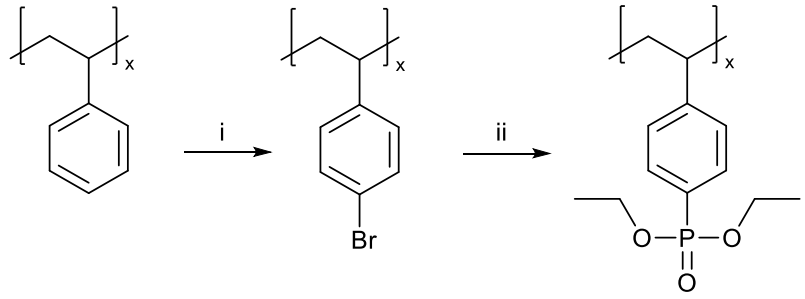
S7. 2D Hirshfeld plots **S14**

S8. Luminescence and lifetime **S16**

S1. Sources of chemicals

Reagent	Manufacturer
4,4'-Dibromo-1,1'-biphenyl	BLDpharm
1,3 diisopropylbenzene	TCI Chemicals
Nickel(II) bromide	Thermos scientific
Triethyl phosphite	Thermos scientific
1,3,6,8-Tetrabromopyrene	BLDpharm
Bis(pinacolato)diboron (B_2pin_2)	BLDpharm
Potassium acetate	AppliChem
$Pd(dppf)Cl_2$	Carbolution
1,4-Dioxane	Fisher Chemical
Magnesium sulphate	VWR Chemicals
Potassium carbonate	Fisher Chemical

S2. Conventional synthetic route of aromatic phosphonates



Scheme S1. General representation of the classical functionalization route (adapted from Subianto et al. [82]). Reagents and conditions: (i) Br_2, $FeCl_3$ (cat.), 1,2-dichloroethane, room temperature, 48 h; (ii) diethyl phosphite ($HPO(OEt)_2$), $Pd(dbac)_3$. Et_3N, diethyl ether, 150 °C, 72 h.

S3. NMR spectra

Diethyl(4'-bromo-[1,1'-biphenyl]-4-yl)phosphonate (**building block A**)

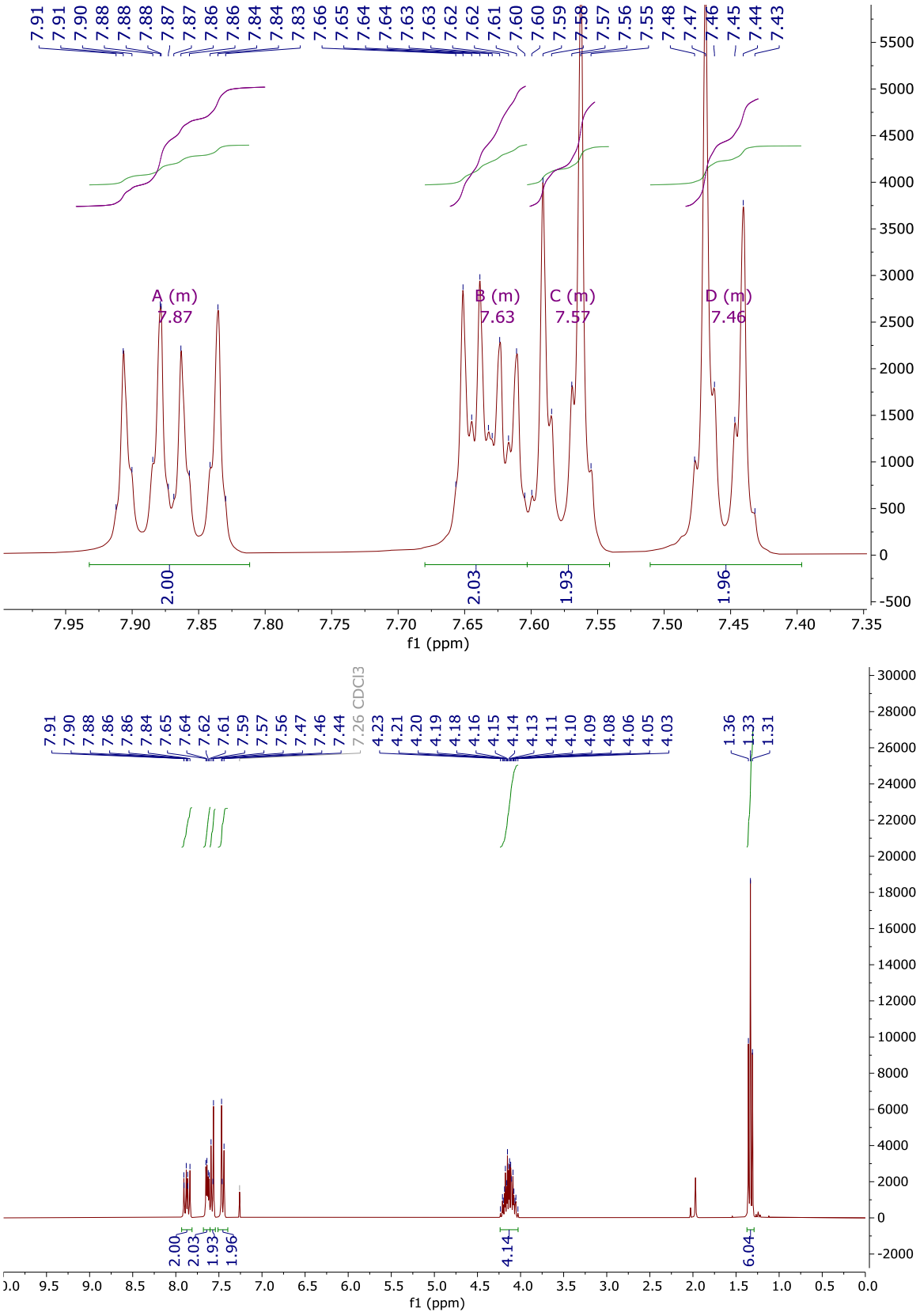


Figure S1. ^{1}H-NMR spectrum (300 MHz) of **building block A** in $CDCl_3$.

1,3,6,8-tetrakis(4,4,5,5-tetramethyl-1,3,2-dioxaborolan-2-yl)pyrene (**building block B**)

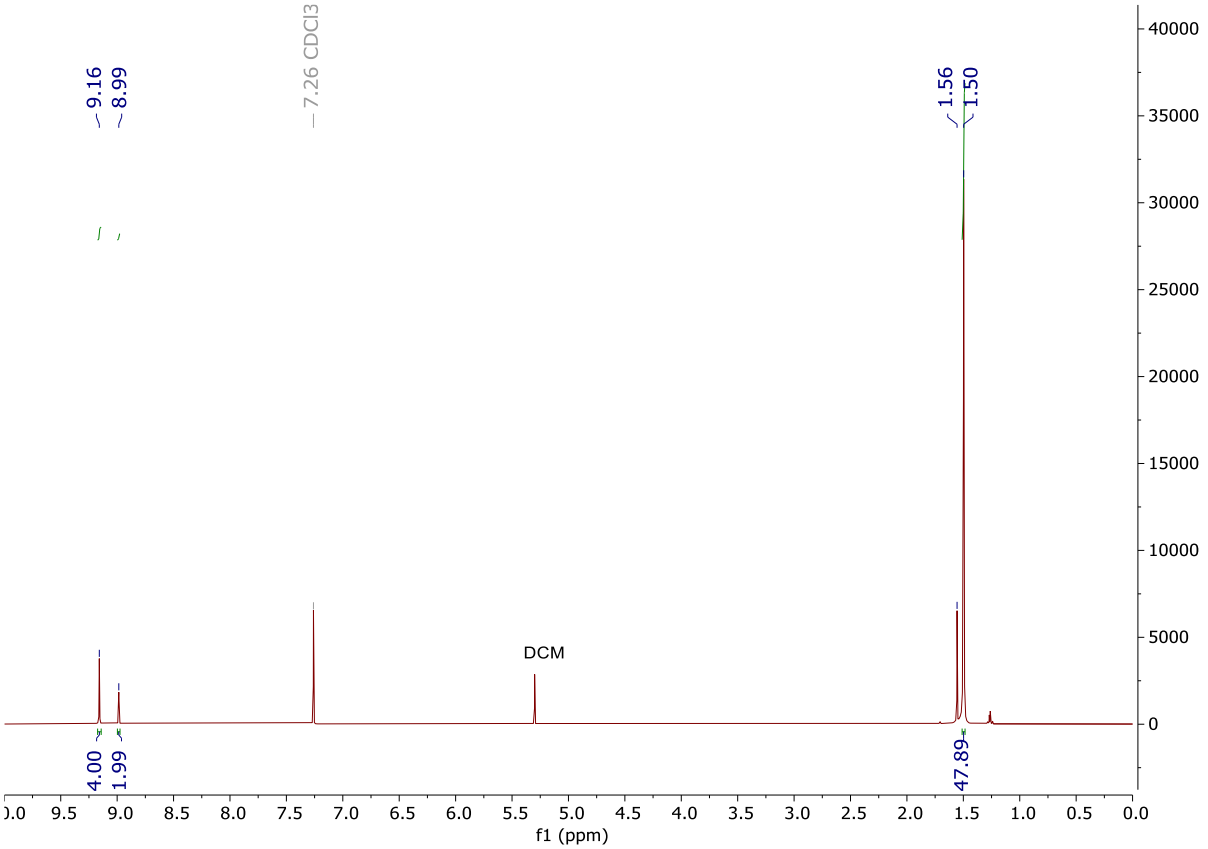


Figure S2. ^{1}H-NMR spectrum (300 MHz) of **building block B** in $CDCl_3$.

Et$_8$-PyTPPE

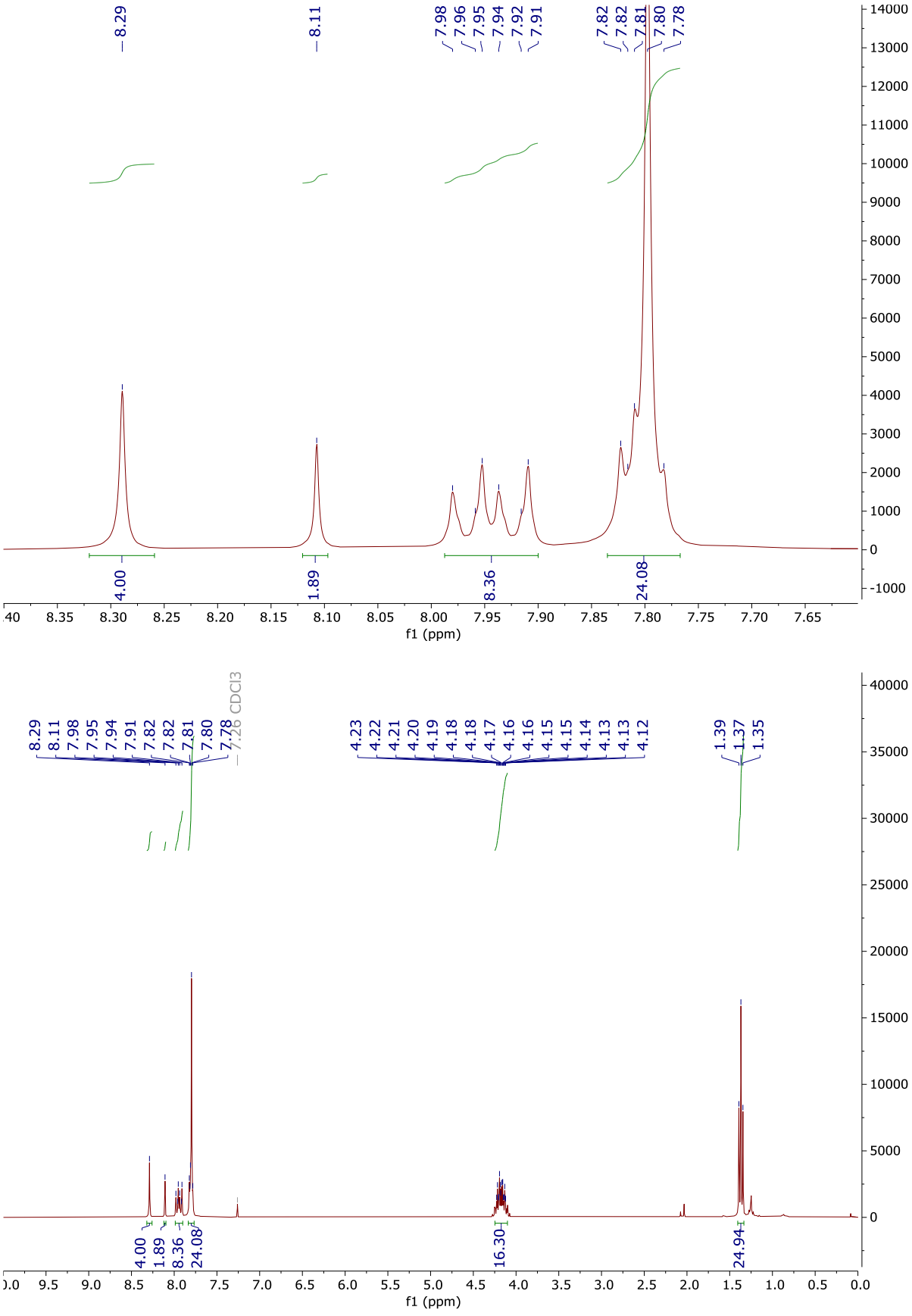


Figure S3. ^{1}H-NMR spectrum (300 MHz) of **Et$_8$-PyTPPE** in $CDCl_3$.

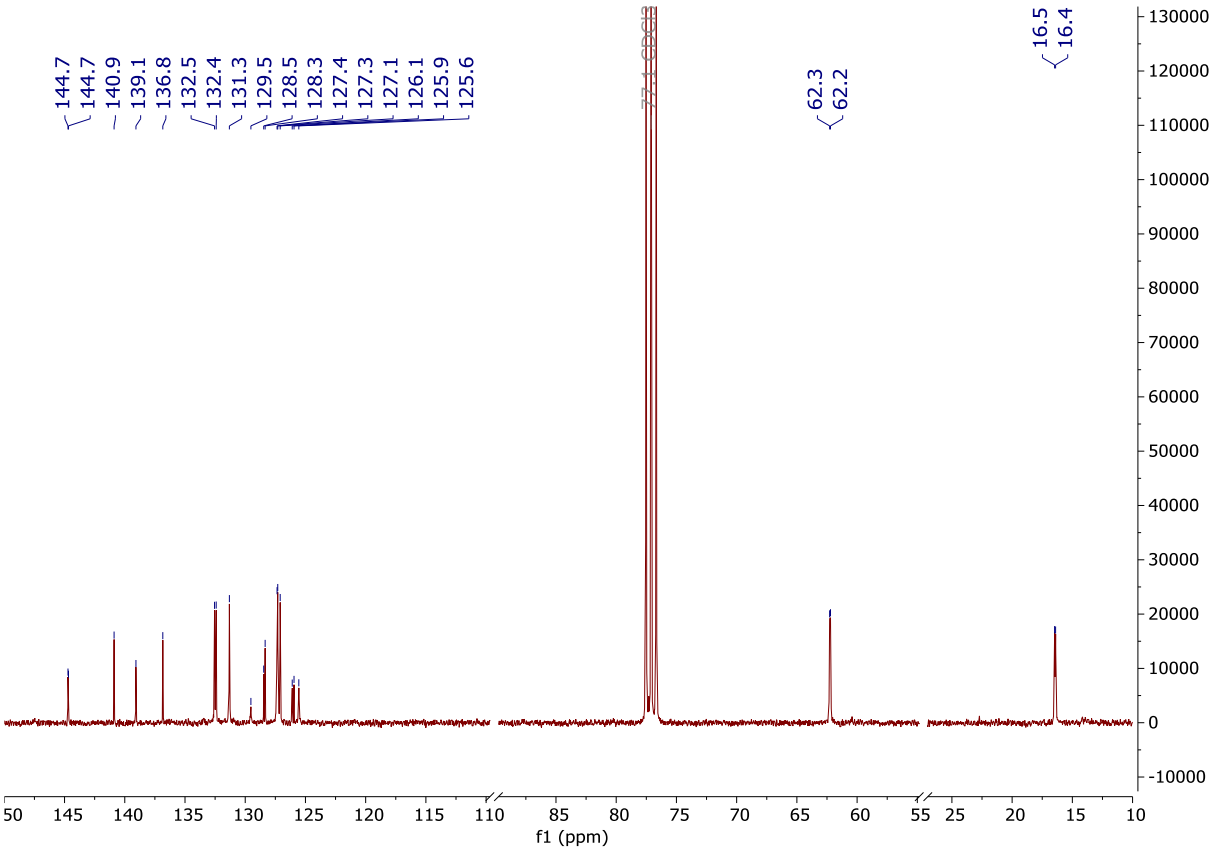


Figure S4. ^{13}C-NMR spectrum (75 MHz) of **Et$_8$-PyTPPE** in $CDCl_3$.

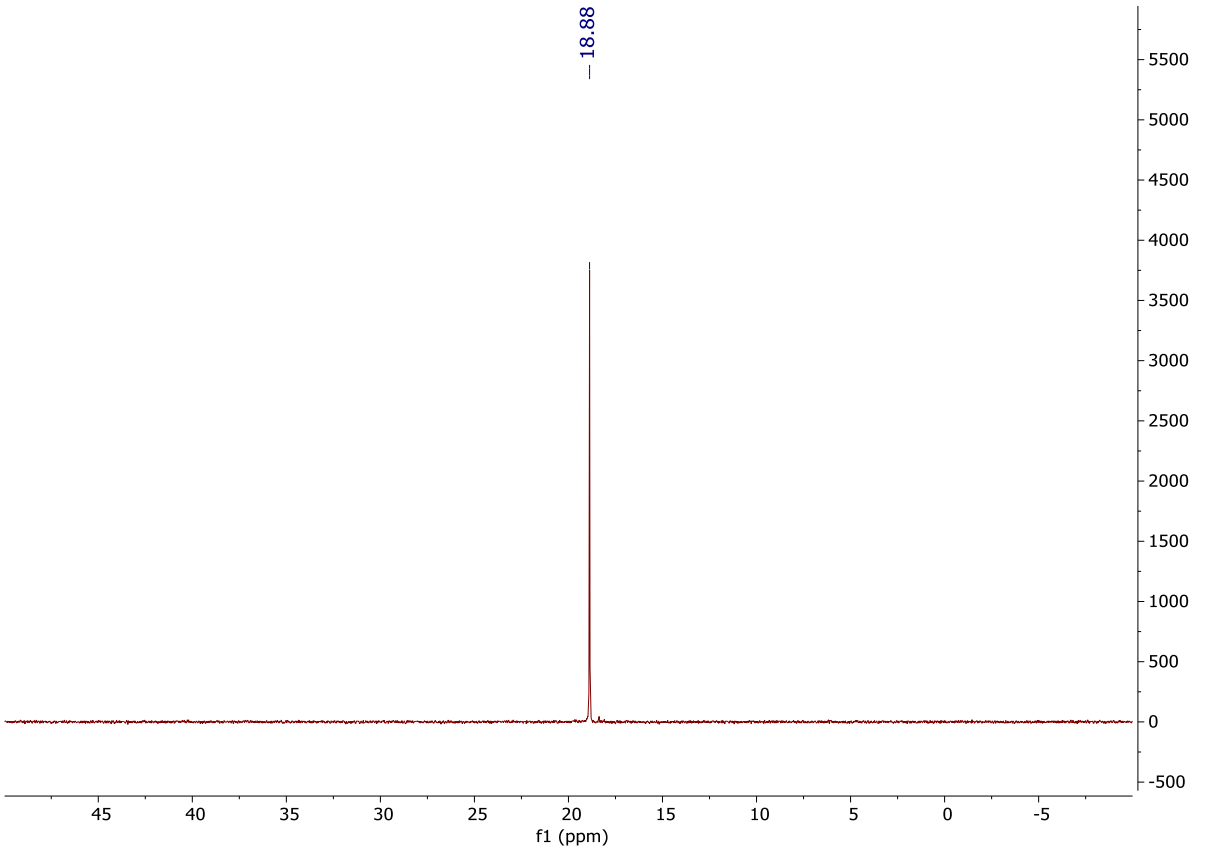


Figure S5. ^{31}P-NMR spectrum (121 MHz) of **Et$_8$-PyTPPE** in $CDCl_3$.

S4. MS spectra

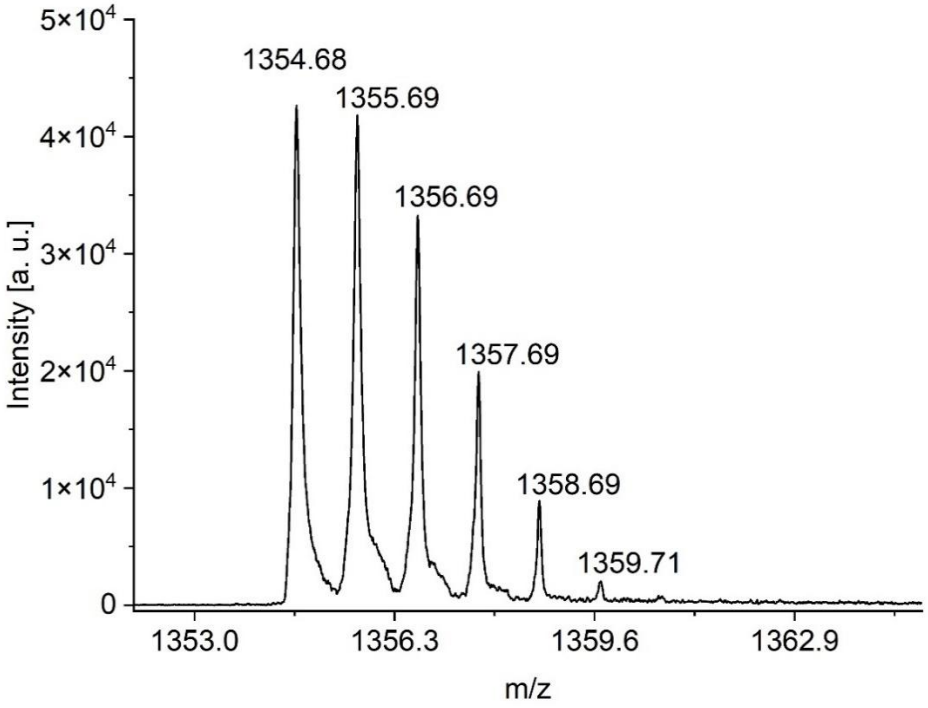


Figure S6. MALDI-TOF-MS of **Et$_8$-PyTPPE** (1354.44 g/mol) with *trans*-2-[3-(4-*tert*-butylphenyl)-2-methyl-2-propenyliden]malononitril as matrix.

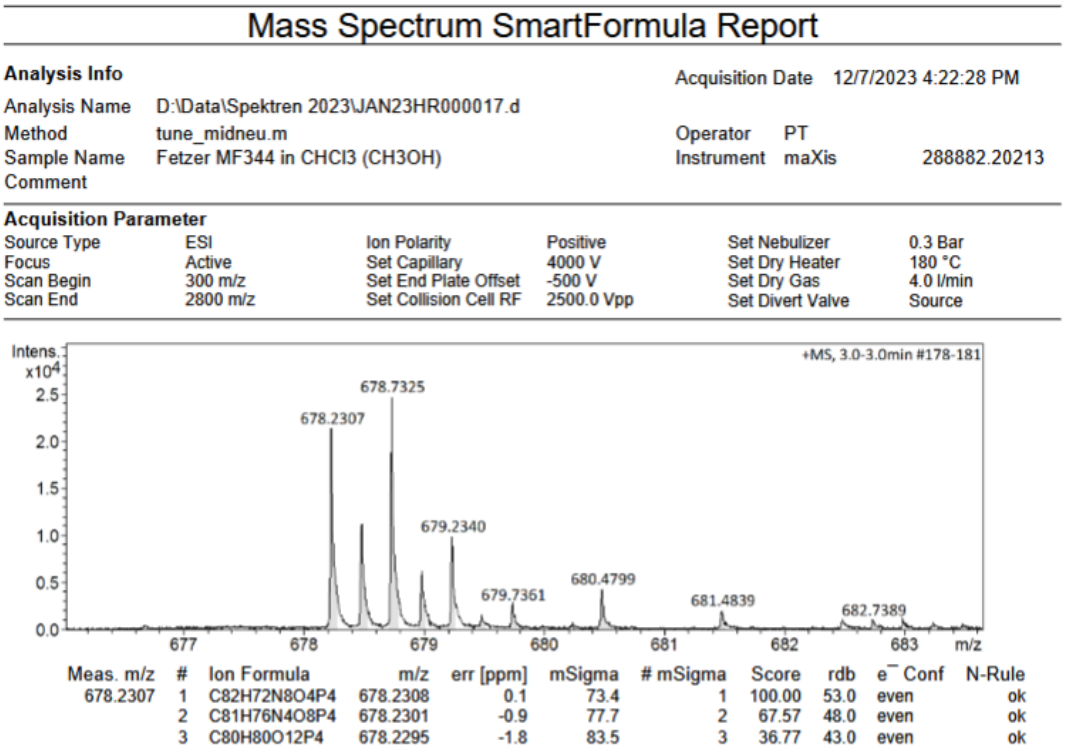


Figure S7. HR-ESI-MS of **Et$_8$-PyTPPE**. Calc. for $[M+2H]^{2+}$: 678.2295 m/z – found: 678.2307 m/z.

S5. X-ray structure of compound Et$_8$-PyTPPE

CCDC reference number is 2472477.

Table S1. Crystal data and structure refinement details for **Et$_8$-PyTPPE**.

Crystal data

$C_{80}H_{78}O_{12}P_4$	Z = 1
M_r = 1355.30	F(000) = 714
Triclinic, $P\bar{1}$	D_x = 1.261 Mg m^{-3}
a = 8.0003 (1) Å	Cu $K\alpha$ radiation, λ = 1.54184 Å
b = 9.3223 (1) Å	Cell parameters from 34962 reflections
c = 24.1656 (3) Å	θ = 3.7–79.1°
α = 95.150 (1)°	μ = 1.48 mm^{-1}
β = 94.929 (1)°	T = 150 K
γ = 93.172 (1)°	Plate, translucent light yellow
V = 1784.77 (4) Å^3	0.46 × 0.21 × 0.16 × 0.12 (radius) mm

Data collection

XtaLAB Synergy, Dualflex, HyPix diffractometer	6530 independent reflections
Radiation source: micro-focus sealed X-ray tube, PhotonJet (Cu) X-ray Source	6224 reflections with $I > 2\sigma(I)$
Mirror monochromator	R_{int} = 0.066 [a]
Detector resolution: 10.0000 pixels mm^{-1}	θ_{max} = 68.2°, θ_{min} = 3.7°
ω scans	h = -9→9
Absorption correction: for a sphere [a] *CrysAlis PRO* 1.171.41.90a (Rigaku Oxford Diffraction, 2020) Spherical absorption correction using equivalent radius and absorption coefficient. Empirical absorption correction using spherical harmonics, implemented in SCALE3 ABSPACK scaling algorithm.	k = -11→11
T_{min} = 0.761, T_{max} = 0.773	l = -29→29
49847 measured reflections	

Refinement

Refinement on F^2	Primary atom site location: dual
Least-squares matrix: full	Hydrogen site location: inferred from neighbouring sites
$R[F^2 > 2\sigma(F^2)]$ = 0.0905 [b] $R[F^2$, all data] = 0.0941	H-atom parameters constrained
$wR[F^2 > 2\sigma(F^2)]$ = 0.1863 [b] $wR(F^2$, all data) = 0.1874	$w = 1/[\sigma^2(F_o^2) + (0.0046P)^2 + 7.9195P]$ where $P = (F_o^2 + 2F_c^2)/3$
S = 1.190 $[F^2 > 2\sigma(F^2)]$ S = 1.191 (F^2, all data)	$(\Delta/\sigma)_{max}$ = 0.001
6530 reflections	$\Delta\rangle_{max}$ = 0.44 e Å^{-3}
457 parameters	$\Delta\rangle_{min}$ = -0.39 e Å^{-3}
69 restraints	

[a] The absorption correction was applied based on the crystal shape. The R_{int} at approximately 7 % is still in the acceptable range. The value reflects the physical characteristics of the sample rather than a processing error. For an efficient measurement, a relatively large crystal was selected, but inherently featured a somewhat lower level of crystallinity. Consequently, the presented dataset represents the best result obtainable for this compound.

[b] The elevated R-factor is rather inherent in this structure. Residual electron density suggests a minor, unresolved rotational disorder within the aromatic core. It is important to note, that the effect is individually too weak, however, the significant number of atoms involved makes the effect perceptible.

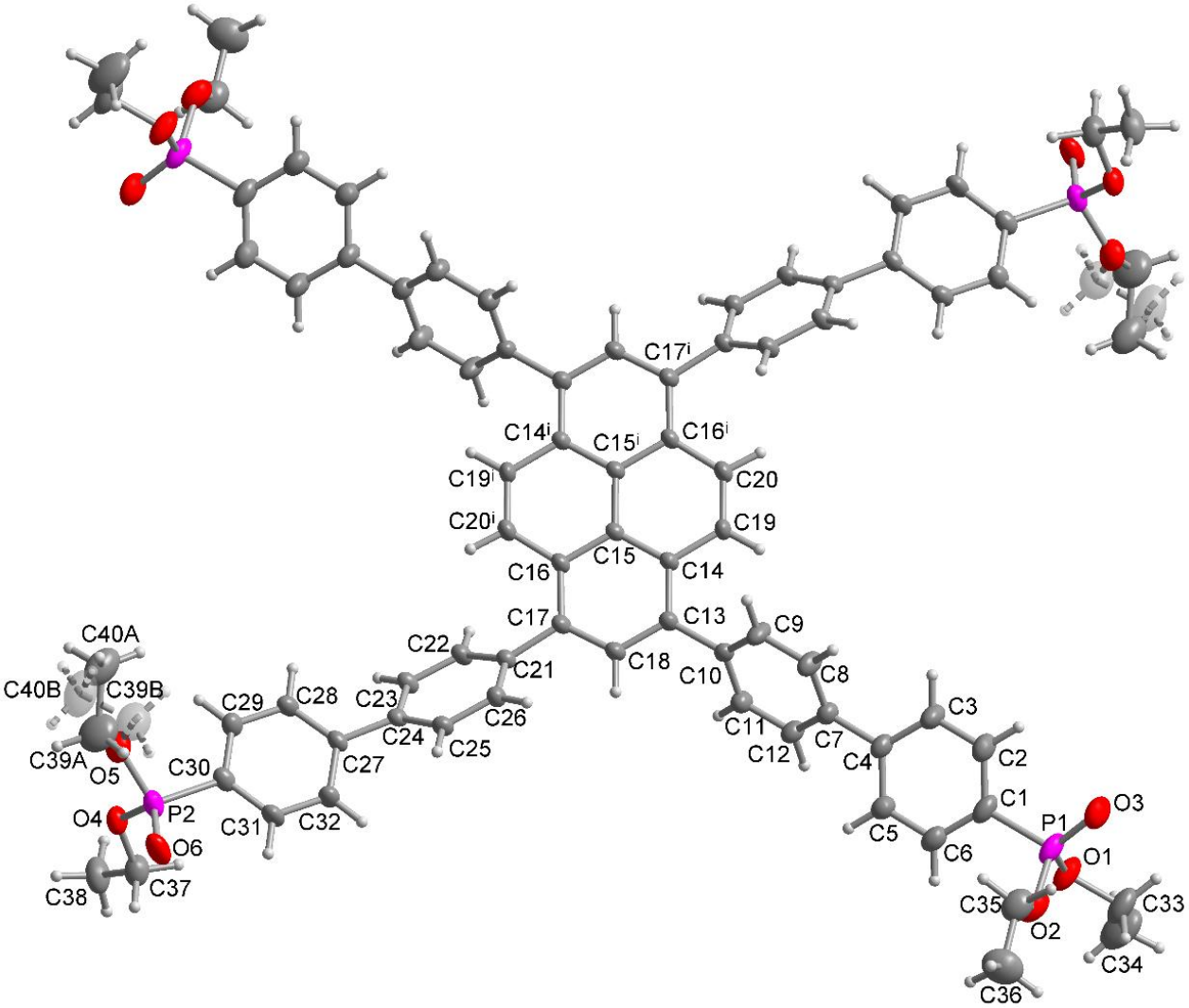


Figure S8. Molecular structure of Et8-PyTPPE in the crystal with atom numbering (50 % thermal ellipsoids; H atoms with arbitrary radii). The CH_2 group (C39) of one of the ethoxy groups at P2 is slightly disordered with the major contributing atom denoted with the suffix A having a site occupation factor (SOF) of 0.54. The minor contribution of the disordered atom has a SOF of 0.46 and is denoted with the suffix B (50 % thermal ellipsoids, H atoms with arbitrary radii). Symmetry code: i = -x+2, -y+2, -z+1.

Table S2. Selected bond distances (Å), bond and interplanar angles (°) for **Et$_8$-PyTPPE** referring to the atom numbering in Figure S8.

P1—O2	1.585 (4)	P2—O4	1.577 (3)
P1—O1	1.569 (4)	P2—O6	1.462 (3)
P1—O3	1.464 (4)	P2—O5	1.572 (4)
P1—C1	1.789 (4)	P2—C30	1.791 (4)
O2—P1—C1	106.5 (2)	O4—P2—C30	106.74 (18)
O1—P1—O2	100.4 (2)	O6—P2—O4	116.5 (2)
O1—P1—C1	102.4 (2)	O6—P2—O5	115.8 (2)
O3—P1—O2	115.8 (2)	O6—P2—C30	111.96 (19)
O3—P1—O1	116.6 (2)	O5—P2—O4	98.04 (19)
O3—P1—C1	113.4 (2)	O5—P2—C30	106.5 (2)

ring	ring	interplanar angle
C7-C8-C9-C10-C11-C12	C13-C14-C15-C16-C17-C18 (pyrene)	60.0 (2)
C1-C2-C3-C4-C5-C6	C7-C8-C9-C10-C11-C12	38.3 (2)
C21-C22-C23-C24-C25-C26	C13-C14-C15-C16-C17-C18 (pyrene)	44.7 (2)
C21-C22-C23-C24-C25-C26	C27-C28-C29-C30-C31-C32	42.9 (2)

S6. π-π stacking and C–H···π interactions

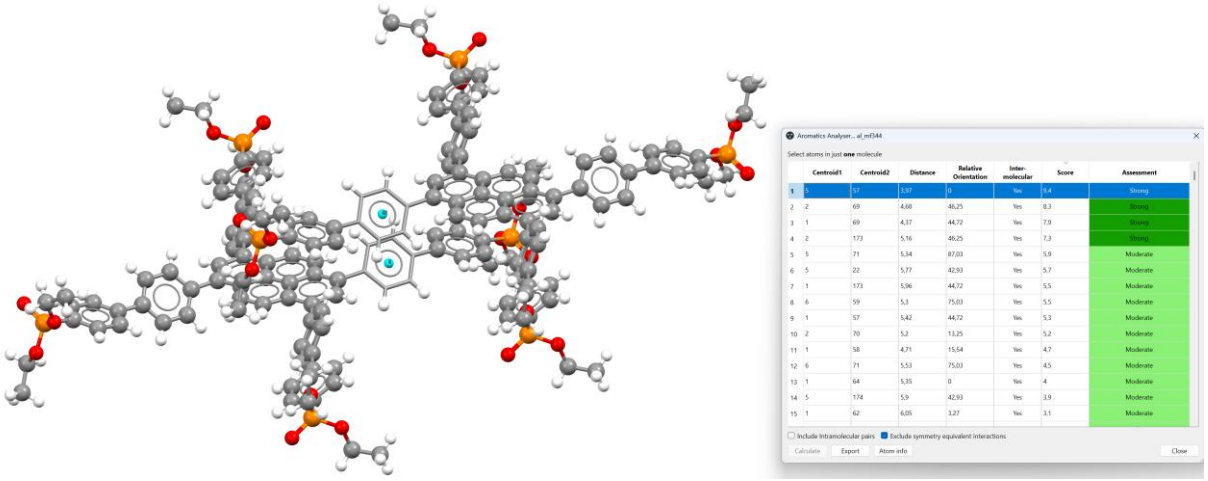


Figure S9. Visual presentation of the π-π stacking interaction from an "Aromatics Analyzer" calculation with the program Mercury [75] in **Et8-PyTPPE**. Despite its classification as "strong" by the Mercury analysis, the centroid-centroid contact of 3.97 Å with parallel ring planes is rather long and weak. Relevant π-π stacking interactions require centroid-centroid contacts of less than 3.8 Å, near parallel ring planes, small slip angles and small vertical displacements (slippage <1.5 Å) which would translate into a sizable overlap of the aryl-plane areas [71,72].

Table S3. Analysis of *inter*molecular C-H...Cg(Pi-Ring) Interactions (H..Cg < 3.0 Ang. - Gamma < 30.0 Deg) in **Et8-PyTPPE**.

- Cg(J) = Center of gravity of ring J (Plane number above)
- H-Perp = Perpendicular distance of H to ring plane J
- Gamma = Angle between Cg-H vector and ring J normal
- C-H..Cg = C-H-Cg angle (degrees)
- C..Cg = Distance of X to Cg (Angstrom)
- C-H, Pi = Angle of the X-H bond with the Pi-plane (i.e.' Perpendicular = 90 degrees, Parallel = 0 degrees)

X--H(I)	Res(I)	Cg(J) [ARU(J)]	H..Cg	H-Perp	Gamma	X-H..Cg	X..Cg	X-H,Pi
C25	-H25	[1] -> Cg4 [2676.01]	2.82	2.81	2.32	130	3.500(4)	37
C25	-H25	[1] -> Cg5 [1455.01]	2.82	2.81	2.32	130	3.500(4)	37
C34	-H34C	[1] -> Cg1 [2777.01]	2.86	2.83	7.85	136	3.627(8)	40
C37	-H37A	[1] -> Cg2 [2566.01]	2.79	2.71	13.73	146	3.659(6)	58
C40	-H40C	[1] -> Cg1 [2576.01]	2.96	2.95	4.84	165	3.911(10)	76

[2676] = 1-X,2-Y,1-Z
[1455] = -1+X,Y,Z
[2777] = 2-X,2-Y,2-Z
[2566] = -X,1-Y,1-Z
[2576] = -X,2-Y,1-Z

Cg1 = centroid of ring C1-C2-C3-C4-C5-C6
Cg2 = centroid of ring C7-C8-C9-C10-C11-C12
Cg4 = centroid of ring C14-C15-C19-C20-C15i-C16i
Cg5 = centroid of ring C15-C16-C14i-C15i-C19i-C20i

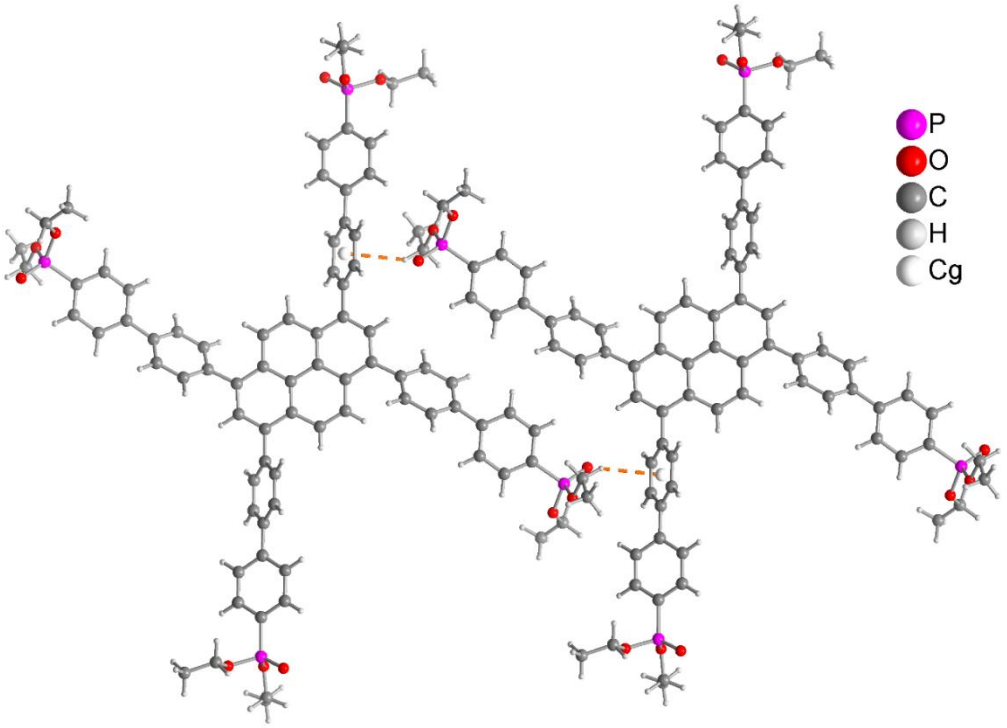
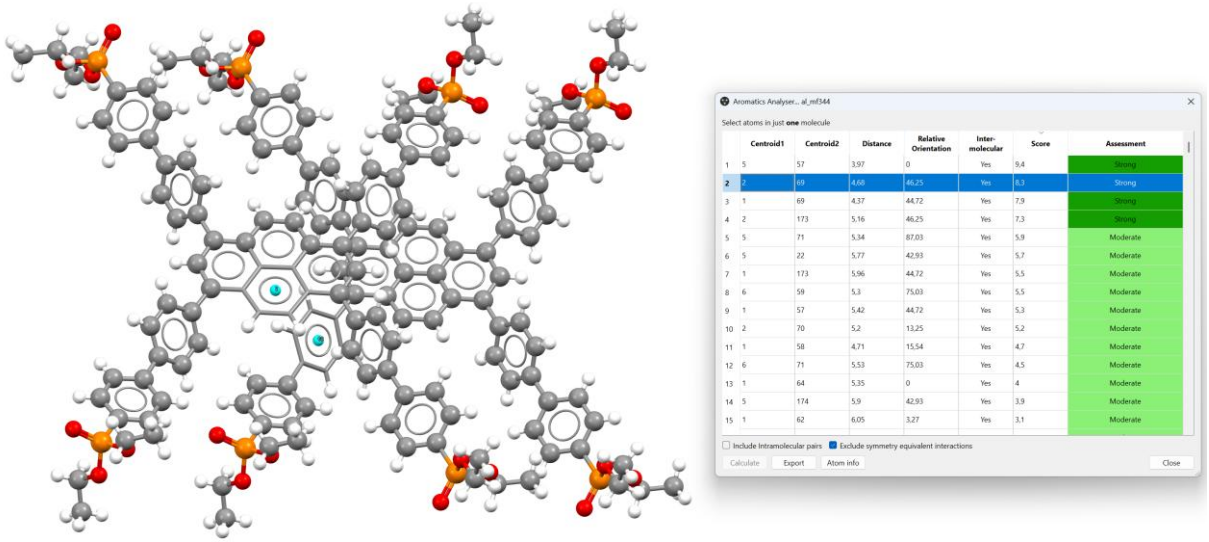


Figure S10. The shortest C-H···π interaction (C37-H37···Cg2) in the packing of **Et$_8$-PyTPPE** in the crystal, indicated as dashed orange lines. Further details of these C-H···π interactions, including the symmetry transformations are listed in the above Table S3 (Cg = ring centroid).



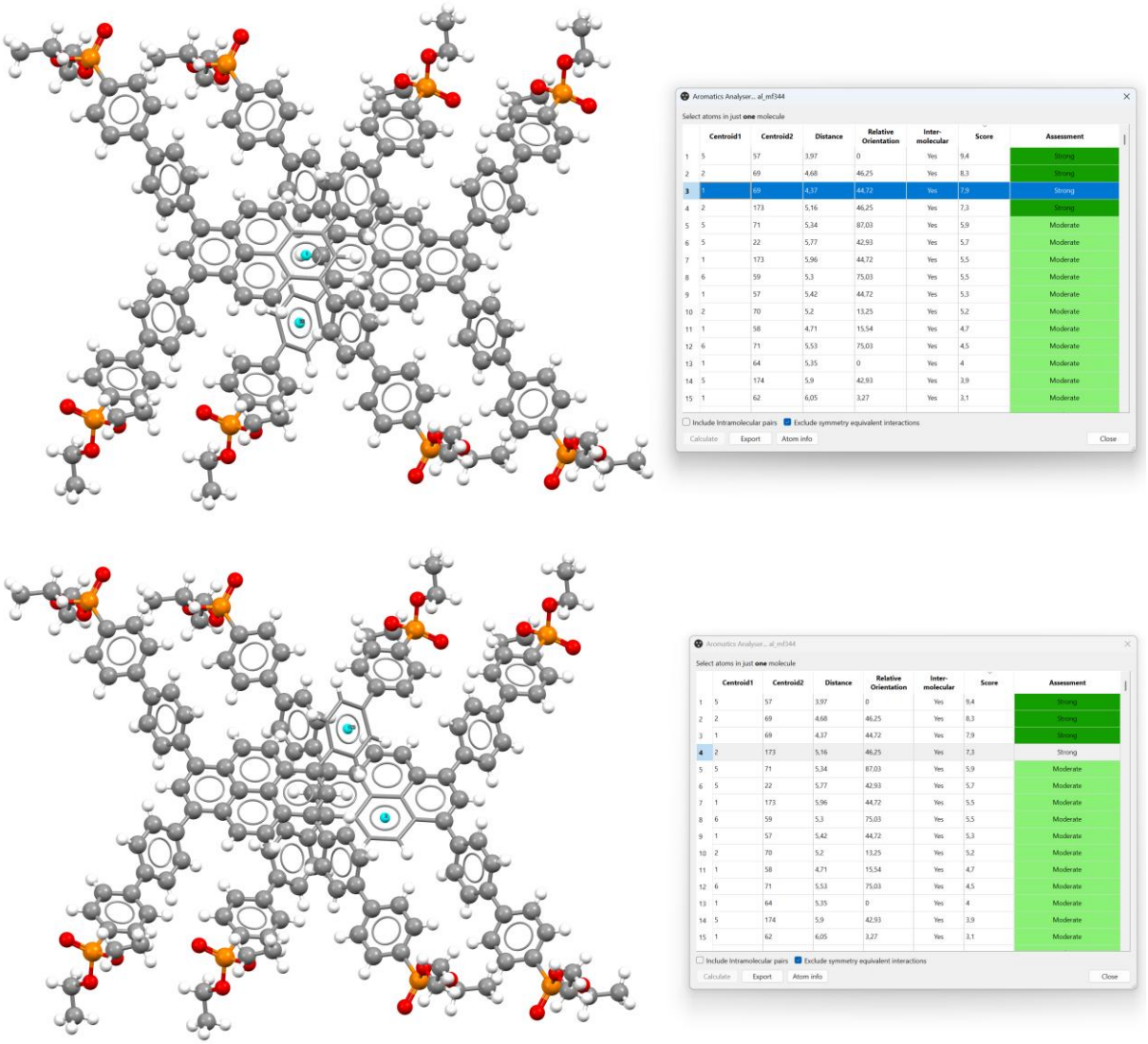


Figure S11. Visual presentation of the three "strong" symmetry-independent aromatic C-H···π interactions from an "Aromatics Analyzer" calculation with the program Mercury [**Error! Reference source not found.**] in the crystal packing of **Et$_8$-PyTPPE**.

S7. 2D Hirshfeld plots

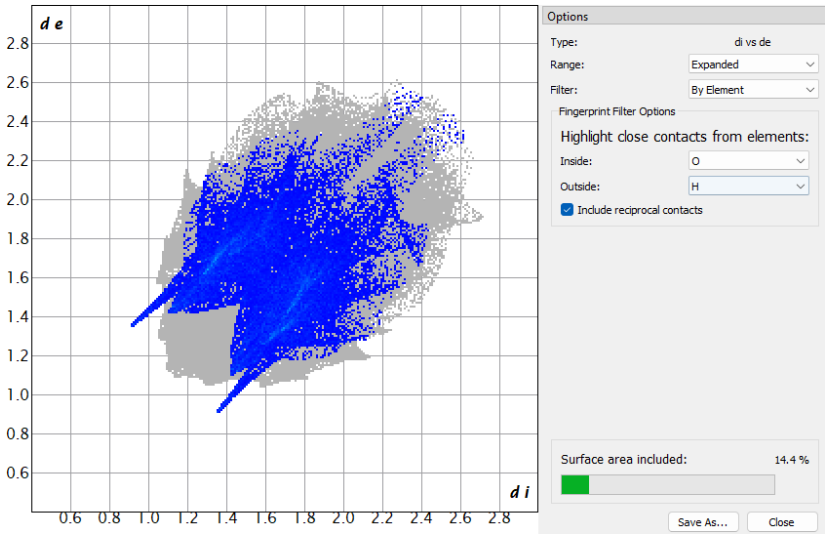


Figure S12. Contribution of O···H contacts in the Hirshfeld 2D plot of **Et$_8$-PyTPPE**.

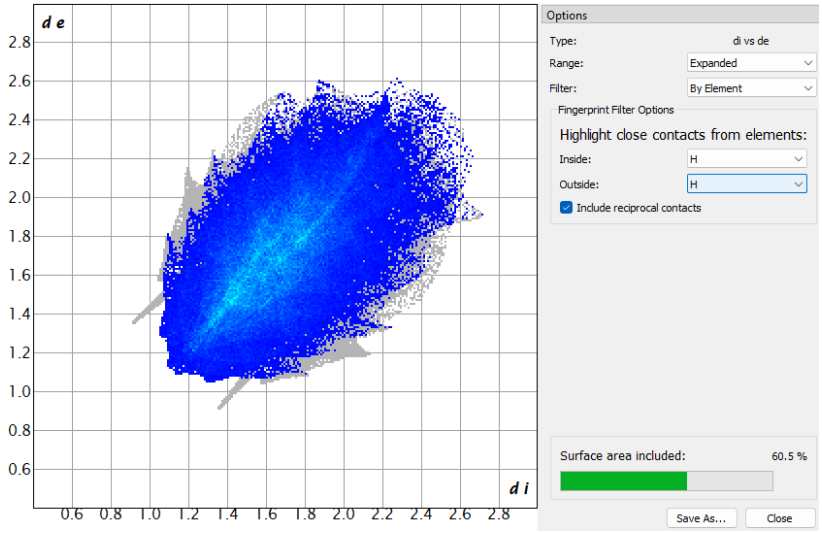


Figure S13. Contribution of H···H contacts in the Hirshfeld 2D plot of **Et$_8$-PyTPPE**.

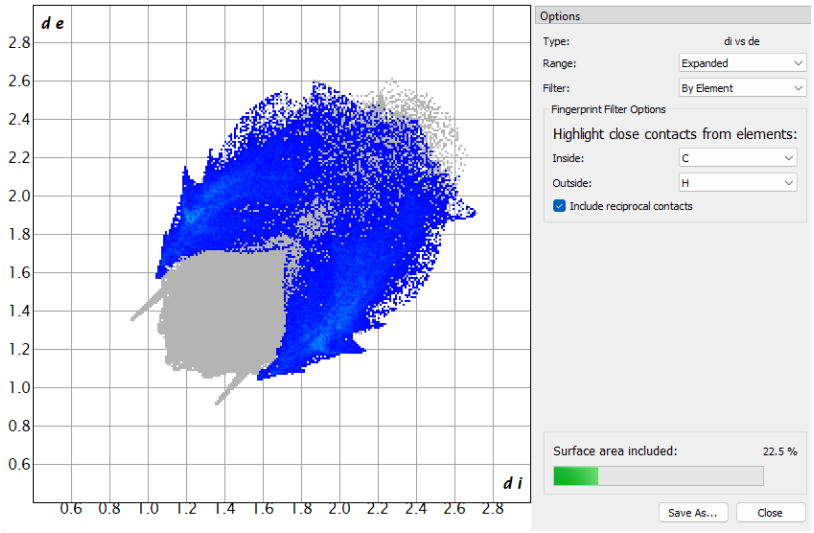


Figure S14. Contribution of C···H contacts in the Hirshfeld 2D plot of **Et$_8$-PyTPPE**.

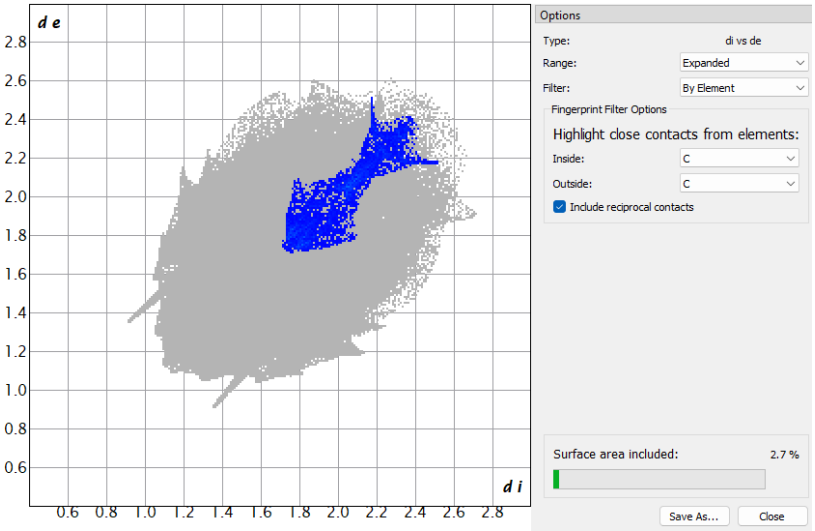
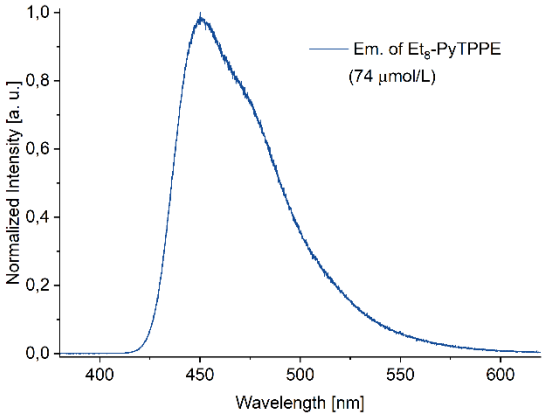
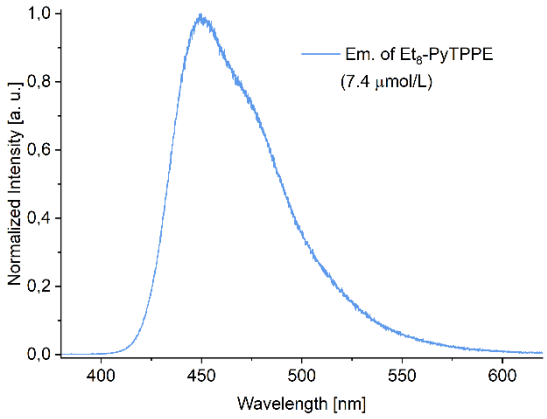


Figure S15. Contribution of C···C contacts in the Hirshfeld 2D plot of **Et$_8$-PyTPPE**.

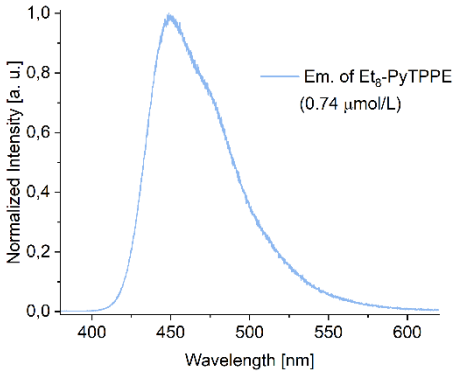
S8. Luminescence and lifetime



(a)



(b)



(c)

Figure S16. Emission measurements using different concentrations of **Et$_8$-PyTPPE** in $CHCl_3$ ($\lambda_{exc.}$ = 375 nm).

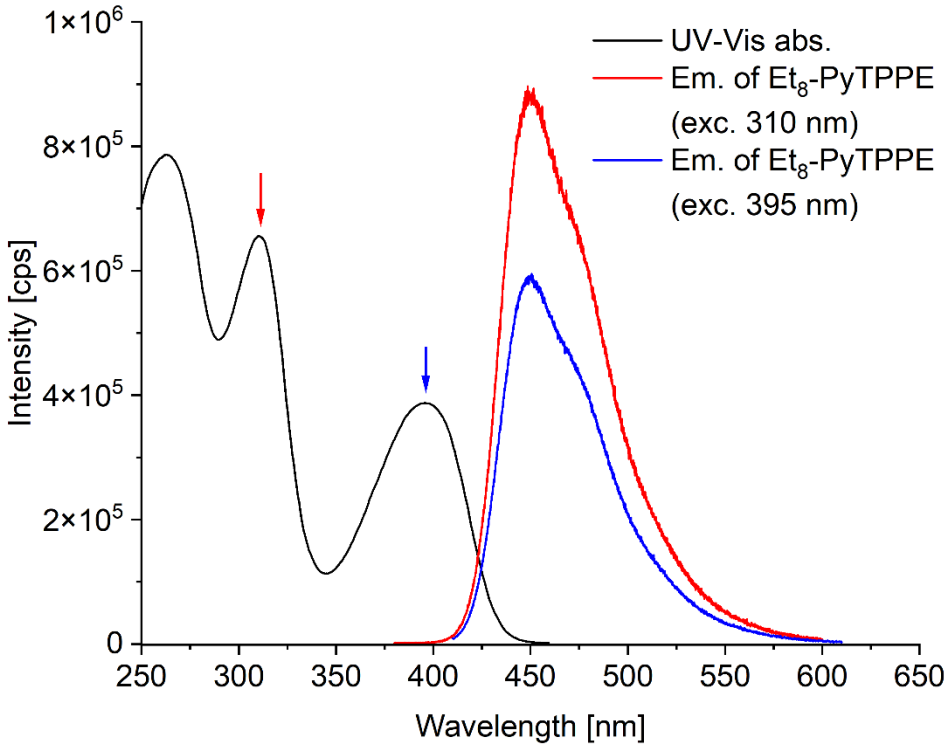


Figure S17. Intensity differences of the emission bands of **Et$_8$-PyTPPE** at the different absorption maxima in $CHCl_3$.

(a) (b)

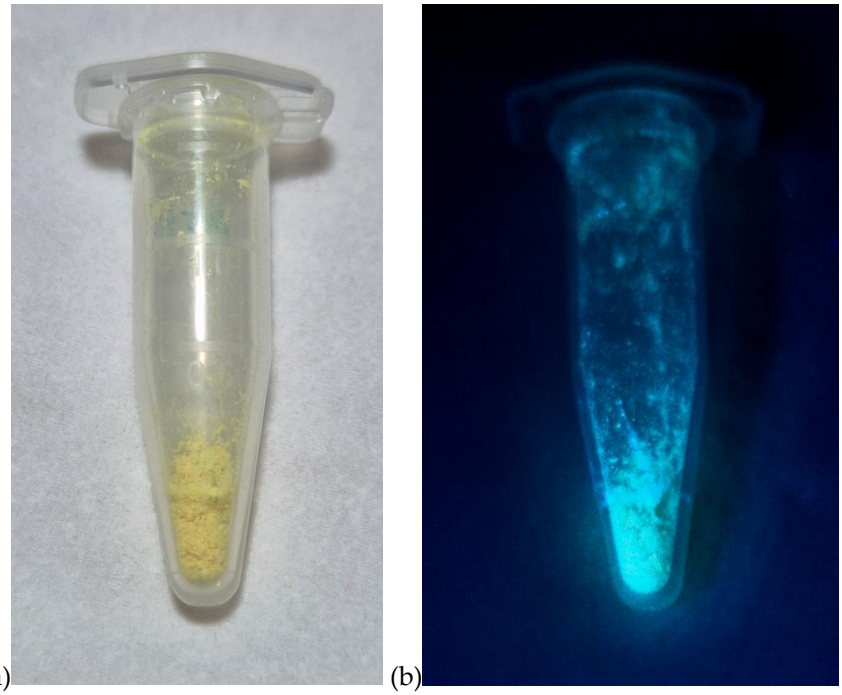


Figure S18. Et$_8$-PyTPPE in solid state under (a) daylight and (b) under UV excitation ($\lambda_{exc.}$ = 365 nm).

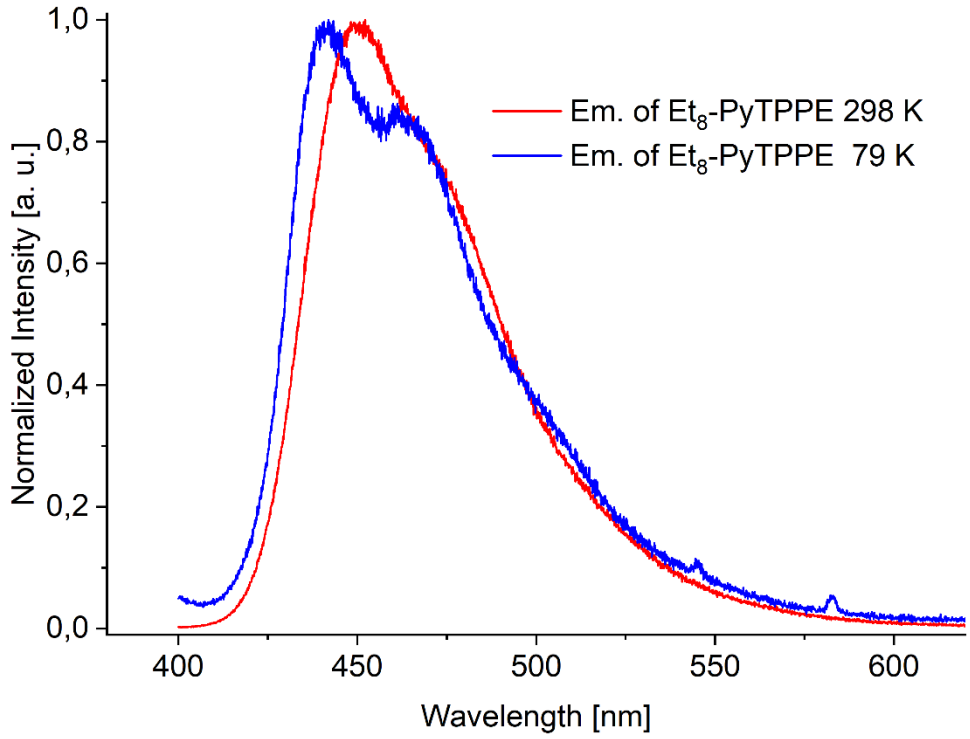


Figure S19. Comparison between 298 K (red) and 79 K (blue) of **Et$_8$PyTPPE** in solution and frozen solution of $CHCl_3$ ($\lambda_{exc.}$ = 375 nm).

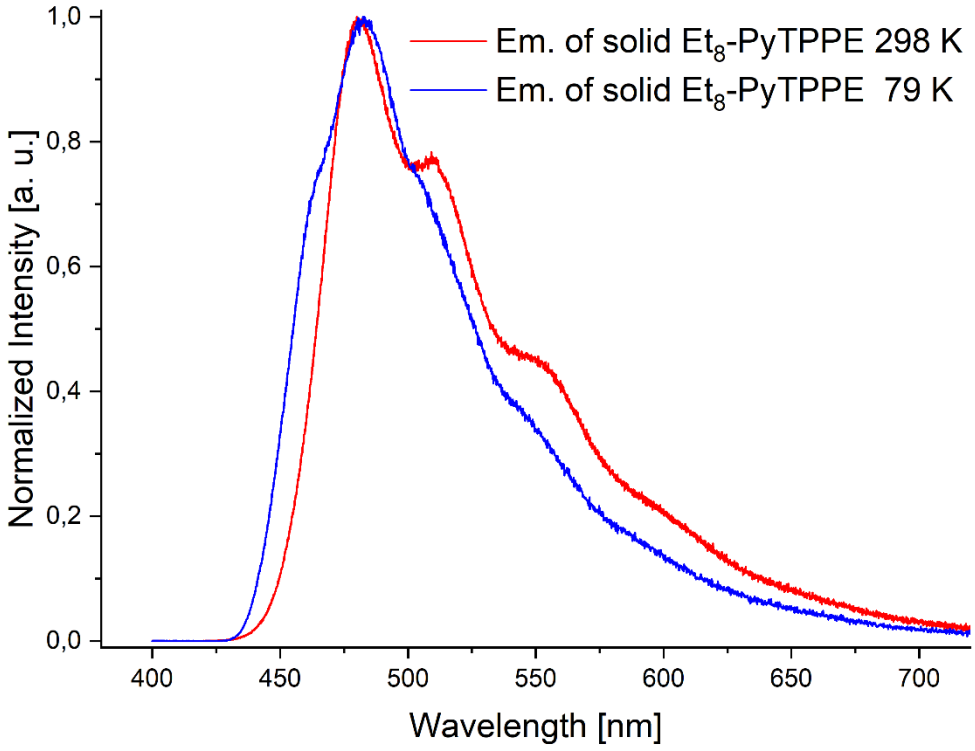


Figure S20. Comparison between 298 K (red) and 79 K (blue) of **Et$_8$PyTPPE** in solid state ($\lambda_{exc.}$ = 375 nm).

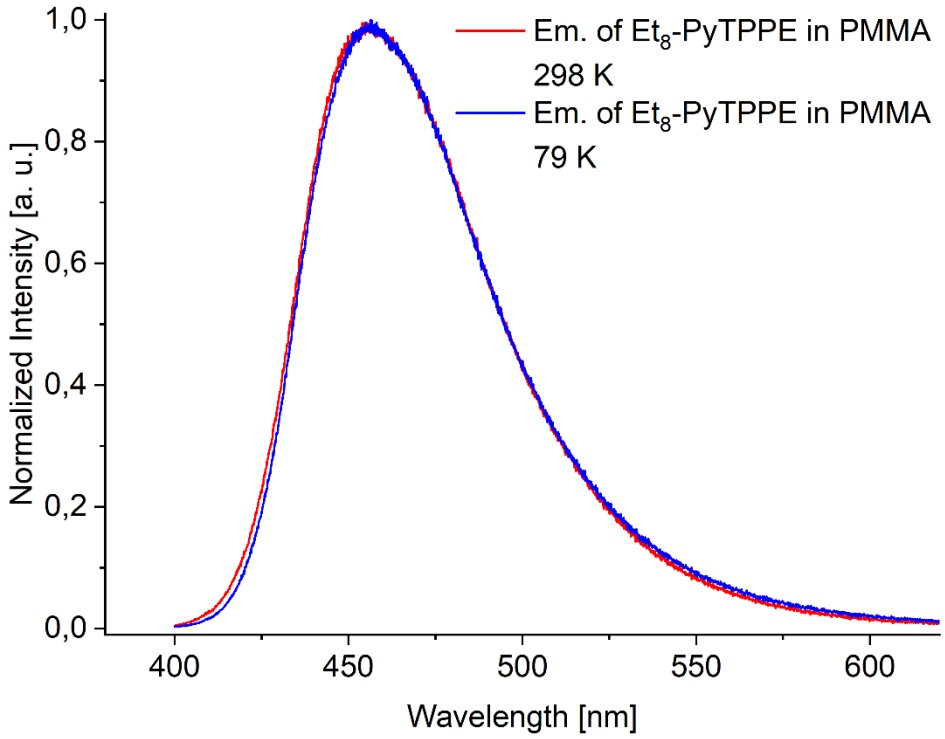


Figure S21. Comparison between 298 K (red) and 79 K (blue) of **Et8PyTPPE** as 1 wt% in a PMMA matrix ($\lambda_{exc.}$ = 375 nm).

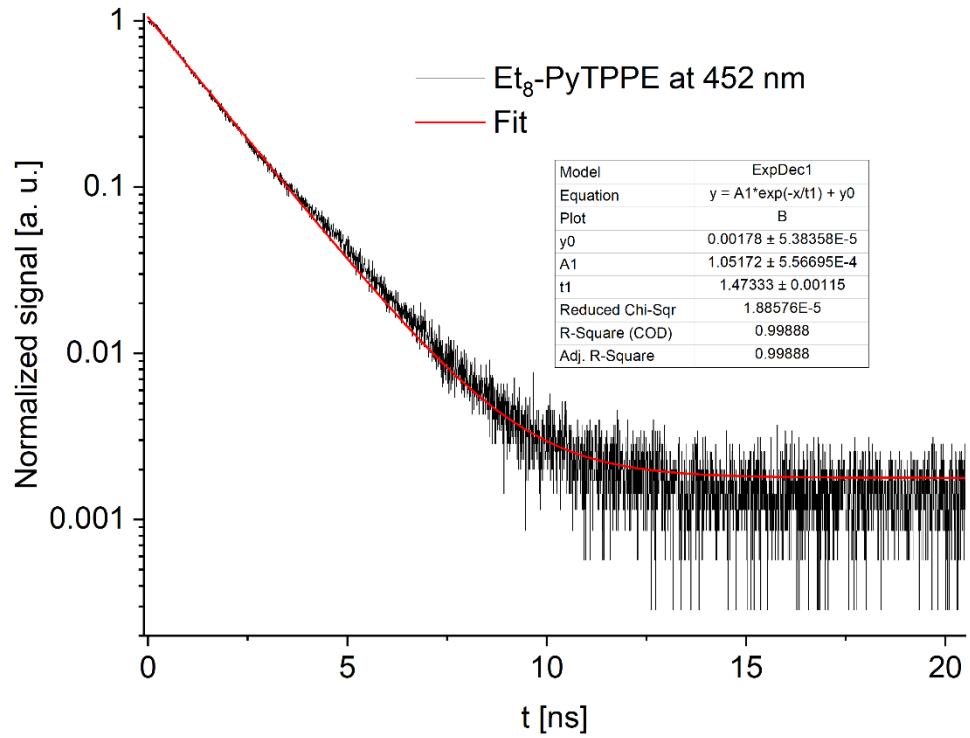


Figure S22. Time-resolved photoluminescence decay (black) of the emission of **Et8-PyTPPE** in $CHCl_3$ solution at 298 K ($\lambda_{exc.}$ = 375 nm) with the fitting parameters, including pre-exponential factor A_i, lifetime t_i, and confidence limits.

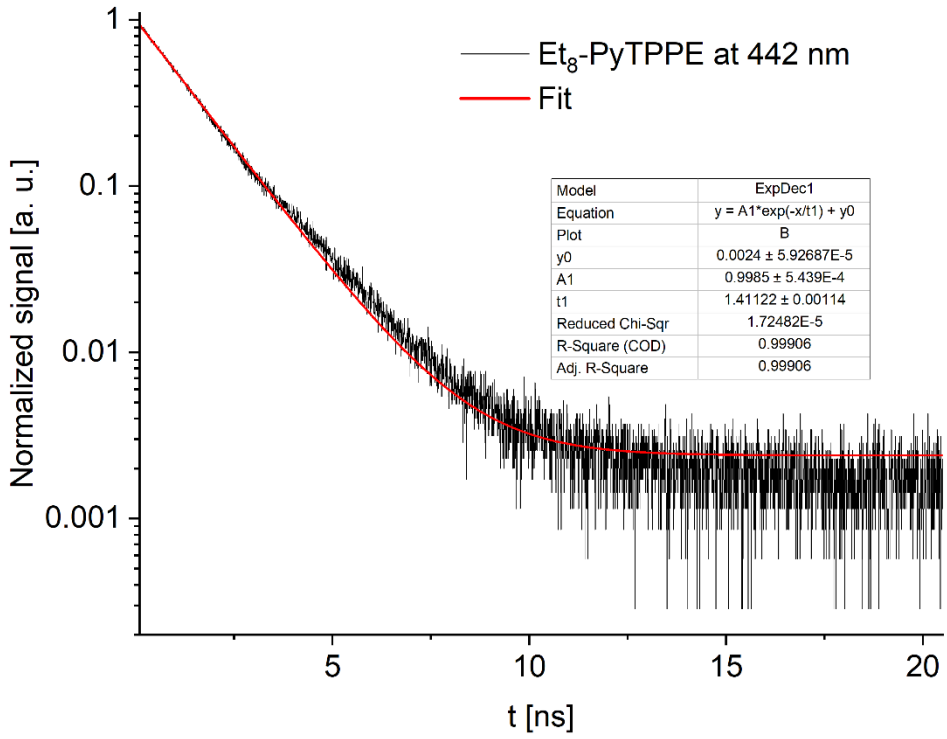


Figure S23. Time-resolved photoluminescence decay (black) of the emission of **Et$_8$-PyTPPE** in $CHCl_3$ solution at 79 K ($\lambda_{exc.}$ = 375 nm) with the fitting parameters, including pre-exponential factor A_i, lifetime t_i, and confidence limits.

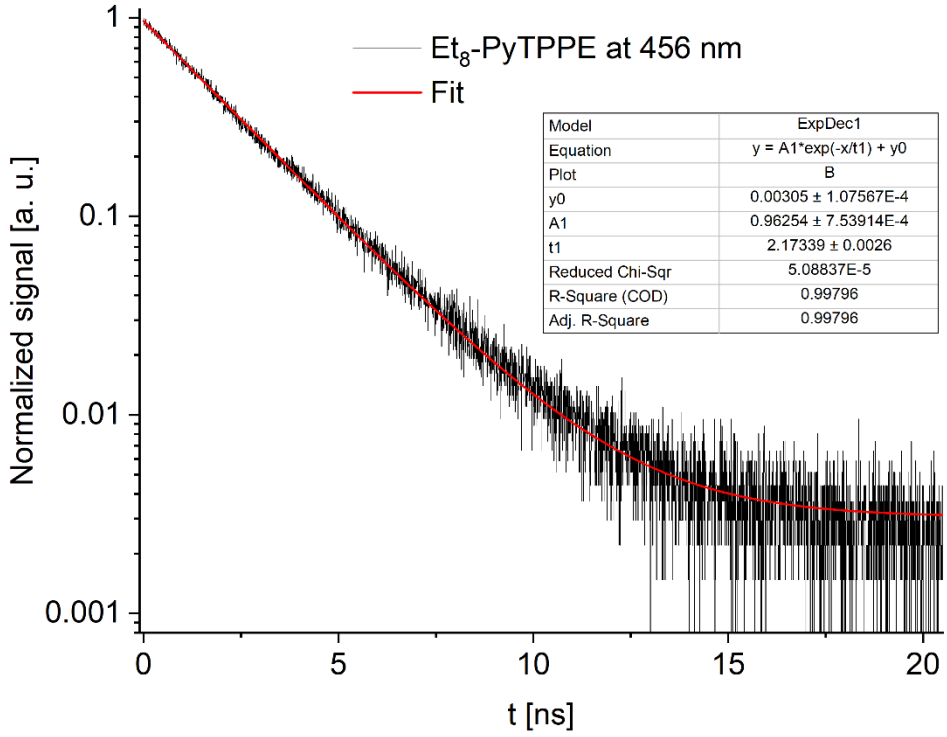


Figure S24. Time-resolved photoluminescence decay (black) of the emission of **Et$_8$-PyTPPE** in PMMA film (1 wt%) at 298 K ($\lambda_{exc.}$ = 375 nm) with the fitting parameters, including pre-exponential factor A_i, lifetime t_i, and confidence limits.

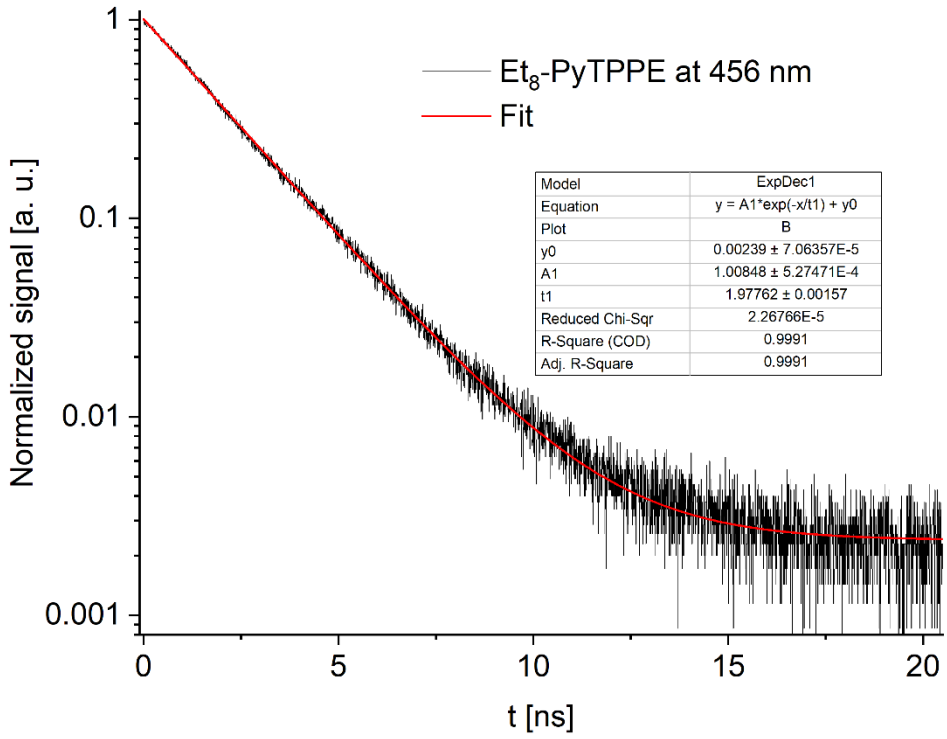


Figure S25. Time-resolved photoluminescence decay (black) of the emission of **Et$_8$-PyTPPE** in PMMA film (1 wt%) at 79 K ($\lambda_{exc.}$ = 375 nm) with the fitting parameters, including pre-exponential factor A_i, lifetime t_i, and confidence limits.

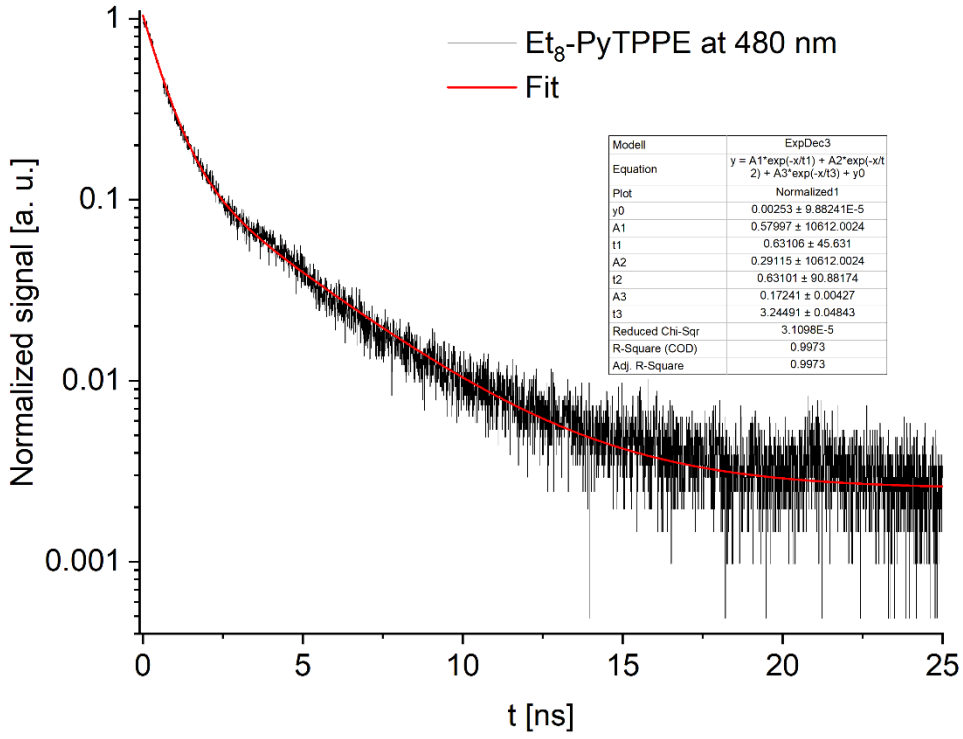


Figure S26. Time-resolved photoluminescence decay (black) of the emission of **Et$_8$-PyTPPE** in the solid state at 298 K ($\lambda_{exc.}$ = 375 nm) with the three-exponential fitting parameters, including pre-exponential factors A_i, lifetimes t_i, and confidence limits.

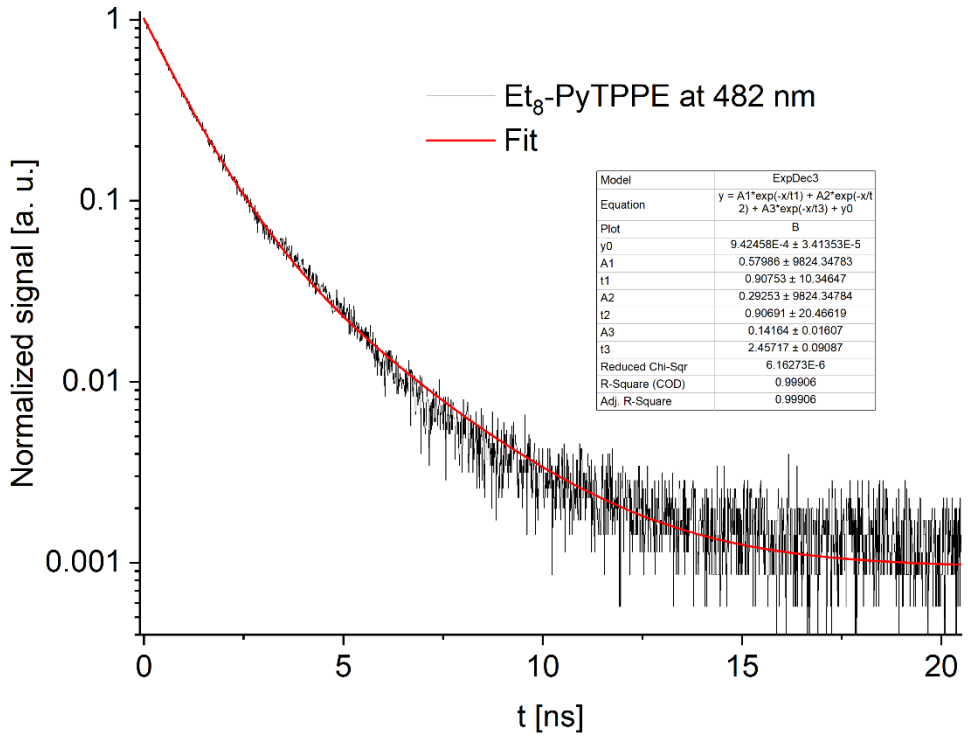


Figure S27. Time-resolved photoluminescence decay (black) of the emission of **Et8-PyTPPE** in the solid state at 79 K ($\lambda_{exc.}$ = 375 nm) with three-exponential fitting parameters, including pre-exponential factors A_i, lifetimes t_i, and confidence limits.